

Fabrication of monodomain alumina pore arrays with an interpore distance smaller than the lattice constant of the imprint stamp

J. Choi, K. Nielsch, M. Reiche, R. B. Wehrspohn,^{a)} and U. Gösele
Max Planck Institute of Microstructure Physics, Weinberg 2, 06120 Halle, Germany

(Received 1 July 2002; accepted 6 January 2003; published 6 March 2003)

Large-area monodomain porous alumina arrays with an interpore distance of 500 nm are fabricated by imprint lithography. A 4 in. imprint master fully compatible with silicon technology was developed, which allows imprint pressures as low as 5 kN/cm² for direct imprint on aluminum. Due to the self-ordering phenomenon of porous alumina growth, we were able to reduce the interpore distance of the pore array to 60% of the lattice constant of the master stamp. Three lithographically defined pores are sufficient to guide anodization of a new pore in the center. © 2003 American Vacuum Society. [DOI: 10.1116/1.1556397]

I. INTRODUCTION

Since the discovery of self-ordered porous alumina in 1995,¹ there has been an ongoing research effort towards new regimes of ordered alumina growth. Up to now, self-ordered alumina structures with 50, 60, 100, 420, and 500 nm interpore distance have been obtained^{2–5} under special conditions defined by the 10% porosity rule.⁶ However, the domain size of self-ordered porous alumina is typically in the range of 20 times the interpore distance and the polydispersity of the pores is about 8%.⁷ For several applications such as photonic crystals,⁸ high density magnetic storage media,⁹ and applications requiring a very monodisperse pore diameters, monodomain pore arrays are necessary. Imprint¹⁰ and electron beam lithography¹¹ have been suggested to obtain monodomain porous alumina structures. However, these methods allow only small imprint areas, typically an electron-beam writing field. Photolithography is normally limited to rather large feature sizes of about minimum 100 nm for the most modern deep-UV stepper.

It was shown initially by Masuda *et al.* that guided anodization of one lithographically missing pore surrounded by six lithographically defined pores occurs when the lattice constant of the holes patterned by lithography matches with self-ordering condition such as the applied potential and the concentration.¹² A similar approach using a commercial grating was carried out by Miskuskas *et al.*¹³ In their work, eight lithographically defined pores guide the anodization of the inner pore in a parallelogram configuration. In this letter, we extend this concept and analyze how many lithographically defined pores are needed to guide anodization. To carry out this study, we first developed an imprint stamp being particularly adapted to hard imprint in aluminum.

II. EXPERIMENT

In the following, the fabrication process of the imprint stamp is briefly described. A master mold for stamping was fabricated from a 4 in. silicon wafer (100). Patterning of a two-dimensional hexagonal array with a lattice constant of

500 nm and a pore diameter of 300 nm was conducted by deep-UV lithography ($\lambda = 248$ nm). Then, inverted pyramids were grown by anisotropic etching the pattern in KOH. A replica of the Si inverted pyramids was obtained by chemical vapor deposition of a Si₃N₄ layer on top of the patterned silicon. The thickness of the Si₃N₄ layer is in the range of 300–500 nm. To obtain a stable stamp, another silicon substrate was wafer bonded^{14,15} on top of the Si₃N₄ layer so that the Si₃N₄ was sandwiched between two silicon substrates. Finally, the initially patterned silicon substrate was removed by grinding and spin etching. Figure 1 shows the master stamp consisting of a hexagonal lattice of pyramids with a

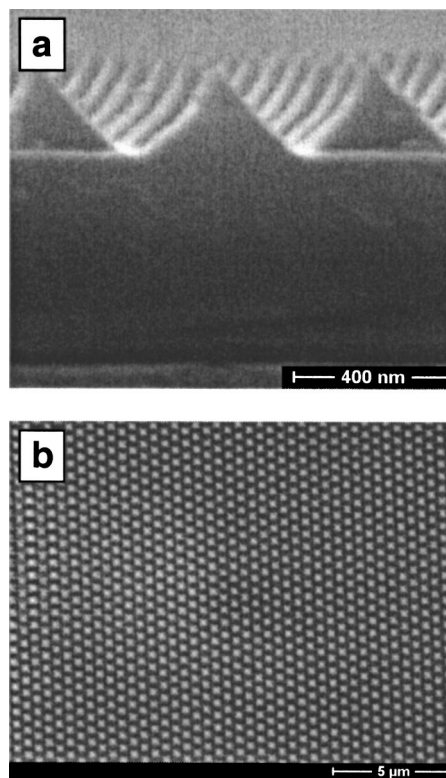


FIG. 1. Scanning electron micrograph of the imprint master consisting of Si₃N₄ pyramids with a 500 nm lattice constant and a 260 nm height; (a) cross section and (b) top view of the imprint master.

^{a)}Author to whom all correspondence should be addressed; electronic mail: wehrspoh@mpi-halle.de

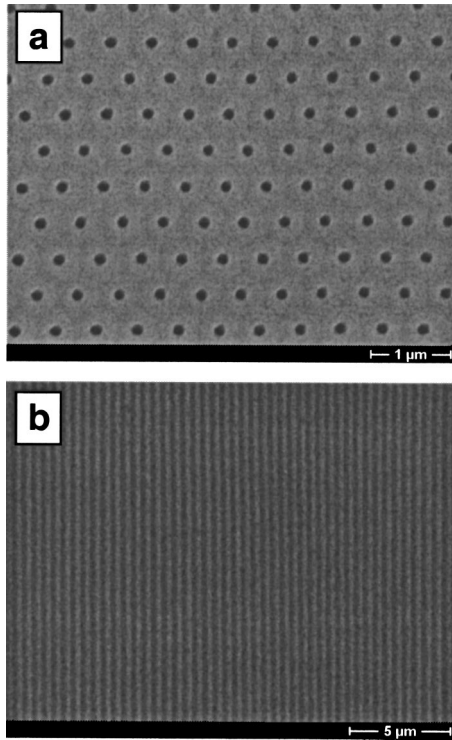


FIG. 2. Scanning electron micrograph of perfectly ordered porous alumina fabricated by anodization of prepatterned aluminum at 195 V in 1 wt % phosphoric acid for 10 h: (a) surface and (b) cross section of porous alumina. The interpore distance is 500 nm corresponding to the lattice constant of the imprint master.

height of about 260 nm and a lattice constant of 500 nm. For the porous alumina preparation, an annealed aluminum sample was mechanically polished to obtain a very smooth surface before imprint (roughness, $R_q < 100$ nm). A piece of 4 in. master stamp (typically, 1×1 cm²) was used and was placed on the electropolished aluminum for the indentation with an oil press (PW, Paul-Otto Weber GmbH).¹⁶ The rectangular shape of the prepatterned holes on the surface of aluminum indicates that the pattern of the master stamp is well transferred. Analysis by atomic force microscopy shows that the depth of the prepattern into aluminum is about 40 nm for an applied pressure of 5 kN/cm². Using a convex pyramid stamp, the stamping pressure required for stable guiding points is about 50 times lower than that of the dot-like master mold fabricated by Masuda *et al.*^{8,10} The prepatterned aluminum substrate is subsequently anodized at the appropriate potential ($D_{\text{int}} = 2.5 \text{ nm/V} \times U$). Note that the interpore distance, D_{int} , of adjacent two pores is determined mainly by the applied potential, U . For example, if the master stamp has a 500 nm lattice constant, anodization should be carried out around 195 V to obtain a 500 nm interpore distance. When self-ordering conditions and prepatterned lattice constant match, very deep pore channels can be obtained over 80 μm, as shown in Fig. 2, which is similar to those obtained by Masuda *et al.*¹⁷

III. RESULTS AND DISCUSSION

The strategy to test how many lithographically defined pores are needed to guide anodization is outlined in Fig. 3.

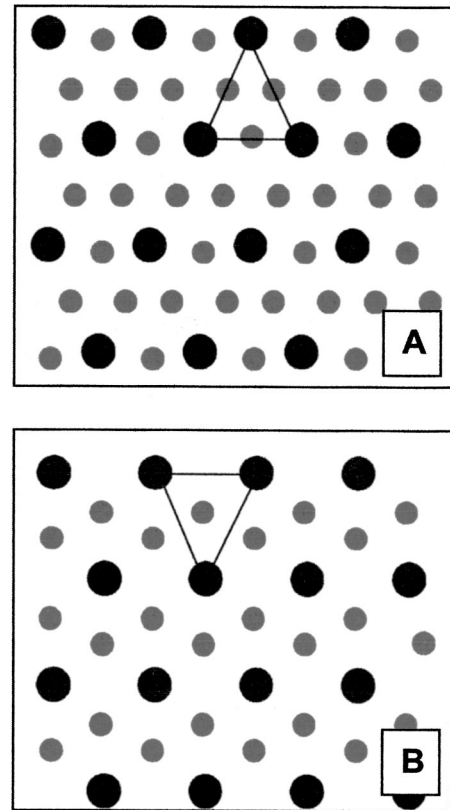


FIG. 3. Schematic diagram of strategies for creating ordered pores in the middle of prepatterned holes without reduction of the lattice constant of the imprint master. Large circles represent prepatterned holes with a 500 nm interpore distance, while small circles correspond to new pores resulting from the self-ordering of porous alumina during the anodization. (A) Two guiding pores to generate new ordered pores in the middle (type A); (B) three guiding pores to generate new pores in the center of the three (type B).

To fabricate new periodic pores in the middle of the prepatterned holes with a 500 nm interpore distance, the anodization was conducted at 100 V (1.7 wt % phosphoric acid, 2 °C, 60 min) corresponding to a $D_{\text{int}}/2 = 250$ nm interpore distance [type A, Fig. 3(a)] or at 120 V (same conditions with 100 V) to obtain an interpore distance of $0.6 \times D_{\text{int}} = 300$ nm [Type B, Fig. 3(b)]. The experimental results for 100 and 120 V are shown in Figs. 4(a) and 4(c), respectively. For type A, new pores that are not made by the stamp initiate irregularly at the boundary of the prepatterned holes as well as in the middle of two prepatterned holes [Fig. 4(a)]. There is also no ordering with depth, as shown in Fig. 4(b). In contrast, for type B, the predicted pores occur in the center of three pores at 120 V anodization potential [Fig. 4(c)]. However, there are some newly initiated pores on unexpected sites between three prepatterned holes. The pores exhibit not all the same size at the beginning of the pore formation. Dissolving selectively the aluminum substrate, the bottom of the pores was investigated [Fig. 4(d)]. An ordered 300 nm pore array is observed, even on large scales [Fig. 4(e)].¹⁸ One cannot distinguish anymore between pores originating from prepatterned and those developed by self-ordering. Some pores must have died or merged during the anodization. Eventually, all the pores tend to be equal in diameter. The coefficient of

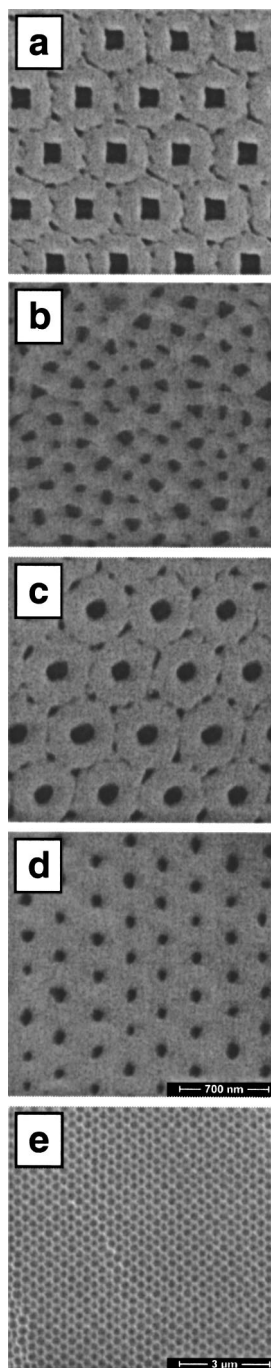


FIG. 4. Realization of strategies suggested in Fig. 3. (a) Top view scanning electron micrograph (SEM) of prepatterned alumina anodized at 2 °C at 100 V in 1.7 wt % phosphoric acid (type A) and (b) bottom view of porous alumina array formed under the conditions for type A. (c) Top view scanning electron micrograph of prepatterned alumina anodized 2 °C at 120 V in 1.7 wt % phosphoric acid (type B). Small (d) and large (e) scale bottom view SEM pictures of the sample of type B exhibiting a perfect hexagonal lattice with 300 nm interpore distance. Note that (e) is slightly widened in 10 wt % phosphoric acid for distinguishing view and the scales of (a), (b), (c), and (d) are the same.

variation of diameter distribution ($C-V$ value = $100 \times$ standard deviation/actual diameter) is 6% as compared to the 2% for Fig. 2(a). The size of pores resulting from the stamp must have decreased, while that of pores formed newly by the

self-ordering must have increased during the anodization. From the above results, it is reasonable to assume that new pores can be guided by three prepatterned points (type B) but not by two prepatterned points (type A). Moreover, we suppose that if there are more than three guiding points on the surface by pre patterning methods, perfectly self-ordered porous alumina in the center of the guiding points can be obtained without the master stamp having a reduced lattice constant. This method would enable for example monodomain pore arrays with an interpore distance of 110 nm for a master stamp of 180 nm or even 36 nm for a stamp of 60 nm, which can be produced by e-beam lithography.¹⁹

Another important aspect of our study is to investigate the change of the pore shape. The shape of pores on the surface depends strongly on the shape of the master mold. For example, a rectangular shape of pores on the surface can be obtained on aluminum indented under high pressure [Fig. 4(a)], whereas a circular shape of the pores on the low-pressured indented aluminum [Fig. 4(c)]. However, the shape of the pores at the bottom is not affected by the shape of prepatterned hole on the surface but by the current flow and the electrolyte.⁶ By comparing surface and bottom view, one observes that the shape of pores indented under high pressure is changed from rectangles into circles during the growth of pores.

IV. CONCLUSION

In conclusion, a new 4 in. silicon imprint stamp consisting of Si_3N_4 pyramids was developed, which is completely compatible with modern silicon processing. Due to the pyramidal shape, the pressure is as low as 5 kN/cm^2 for direct indentation on aluminum. Furthermore, based on the self-ordering phenomenon of alumina, we could reduce the interpore distance of porous alumina to 60% of the lattice constant of the master stamp. We obtained perfectly ordered porous alumina with 300 nm interpore distance by means of a 500 nm periodic master stamp. This is a route to obtain monodomain alumina templates with interpore distances smaller than that of the master and the lithographic limit.

ACKNOWLEDGMENTS

The authors wish to thank S. Hopfe and B. Lausch for technical support and Dr. M. Alexe for stimulating discussions concerning the imprint master.

¹H. Masuda and K. Fukuda, *Science* **268**, 1466 (1995).

²H. Masuda, F. Hasegawa, and S. Ono, *J. Electrochem. Soc.* **144**, L127 (1997).

³O. Jessensky, F. Müller, and U. Gösele, *Appl. Phys. Lett.* **72**, 1173 (1998).

⁴A.-P. Li, F. Müller, A. Birner, K. Nielsch, and U. Gösele, *J. Appl. Phys.* **84**, 6023 (1998).

⁵H. Masuda, K. Yada, and A. Osaka, *Jpn. J. Appl. Phys., Part 2* **37**, L1340 (1998).

⁶K. Nielsch, J. Choi, K. Schwirm, R. B. Wehrspohn, and U. Gösele, *Nano Lett.* **2**, 677 (2002).

⁷R. B. Wehrspohn, A. P. Li, K. Nielsch, F. Müller, W. Erfurth, and U. Gösele, in *Oxide Films*, edited by K. R. Hebert, R. S. Lillard, and B. R.

- Mac Dougall, PV-2000-4 (Electrochemical Society, Pennington, NJ, 2000), p. 271.
- ⁸H. Masuda, M. Ohya, H. Asoh, M. Nakao, M. Nohtomi, and T. Tamamura, *Jpn. J. Appl. Phys., Part 2* **38**, L1403 (1999).
- ⁹K. Nielsch, R. B. Wehrspohn, J. Barthel, J. Kirschner, U. Gösele, S. F. Fischer, and H. Kronmüller, *Appl. Phys. Lett.* **79**, 1360 (2001).
- ¹⁰H. Masuda, H. Yamada, M. Satoh, H. Asoh, M. Nakao, and T. Tamamura, *Appl. Phys. Lett.* **71**, 2770 (1997).
- ¹¹A.-P. Li, F. Müller, and U. Gösele, *Electrochem. Solid-State Lett.* **3**, 131 (2000).
- ¹²H. Masuda, M. Yotsuya, M. Asano, K. Nishio, M. Nakao, A. Yokoo, and T. Tamamura, *Appl. Phys. Lett.* **78**, 826 (2001).
- ¹³I. Mikulskas, S. Juodkazis, R. Tomašiūnas, and J. G. Dumas, *Adv. Mater.* **13**, 1574 (2001).
- ¹⁴Q. Y. Tong and U. Gösele, *Adv. Mater.* **11**, 1409 (1999).
- ¹⁵A. Plöbl and G. Kräuter, *Mater. Sci. Eng., R.* **25**, 1 (1999).
- ¹⁶www.p-o-weber.de
- ¹⁷H. Asoh, K. Nishio, M. Nakao, T. Tamamura, and H. Masuda, *J. Electrochem. Soc.* **148**, B152 (2001).
- ¹⁸M. Alexe, J. Choi, U. Gösele, K. Nielsch, M. Reiche, and R. B. Wehrspohn, Germany Patent Application No. DE10207952.8 (2002).
- ¹⁹H. Asoh, K. Nishio, M. Nakao, A. Yokoo, T. Tamamura, and H. Masuda, *J. Vac. Sci. Technol. B* **19**, 569 (2001).